Adsorption of textile dyes on raw Tunisian clay: Equilibrium, kinetics and thermodynamics

Nahed naghmouchi and kais nahdi*

Laboratoire d'Application de la Chimie aux Ressources et Substances Naturelles et à l'Environnement (LACReSNE), Université de Carthage, Faculté des Sciences de Bizerte, 7021 Zarzouna, Bizerte, Tunisia

k_nahdi@yahoo.fr

ABSTRACT

Natural clay from Nabeul region (north of Tunisia) was investigated for the removal of two anionic textile dyes (RR120 and BB150) from aqueous solution. The raw clay was characterized by means of XRD, IR spectroscopic, chemical analysis, cation exchange capacity and BET surface area analysis.

Adsorption studies were carried out under various parameters such as pH, contact time, initial dye concentration and temperature. The adsorption kinetic data was tested by pseudo-first order, pseudo second-order and intra-particle diffusion kinetic models. The equilibrium data were analyzed using Langmuir, Freundlich, Temkin and Dubinin–Radushkevich isotherm models. The thermodynamic parameters ($\Delta H°$, $\Delta S°$ and $\Delta G°$) of the adsorption were also evaluated. The adsorption process was found spontaneous and endothermic in nature. The kinetics of adsorption were best described by pseudo-second order kinetic model. The Langmuir adsorption model totally agrees with the experimental data.

Keywords

Tunisian clay, Adsorption isotherm, Textile dyes, thermodynamic

Academic Discipline And Sub-Disciplines

chemistry

SUBJECT CLASSIFICATION

Chemistry subject classification

TYPE (METHOD/APPROACH)

Experimental study

Council for Innovative Research

Peer Review Research Publishing System

Journal: Journal of Advances in Chemistry

1. INTRODUCTION

Water contamination by pollutants from various sources is a current problem. Especially in the textile industry, wastewater is one of the largest sources of surface water and groundwater pollution. Because of the high stability and the low biodegradability of textile dyes they cause serious environmental problems. Among 7.10^5 t and approximately 10,000 different types of dyes and pigments produced worldwide annually, it is estimated that 1–15% of the dyes are lost in the effluents during the dyeing process [1]. Thus it is imperative to treat the wastewater from the textile industries before they are discharged into the sewer system.

The treatment of water contaminated by textile dyes was the subject of several studies to reduce the color intensity and the amount of organic matter. Several decontamination methods have been developed, we cite as examples: adsorption [2,3], ion exchange [4,5], flocculation-coagulation [6]…etc.

Many adsorbents have been tested to reduce dye concentrations from aqueous solutions such as activated carbon [7], adsorbents including agricultural wastes [8,9], lignite [10], natural phosphate [11], chitosan [12], silica [13], kaolinite [14], hydroxyapatite [15,16], perlite [17], sepiolite [18], montmorillonite [19] and some natural biosorbents have also been reported [20,21].

However, the use of natural materials is a promising alternative due to their relative abundance and low commercial value.

The present work concerns the study of the potentiality of Tunisian natural clay as a low cost adsorbent for the removal of two organic textile dyes from aqueous solution as an ideal alternative to the current expensive methods of removing dyes from wastewater.

Adsorption studies were carried out under various parameters such as pH, contact time, initial dye concentration and adsorption temperature. The adsorption kinetic data was tested by pseudo-first-order, pseudo-second-order and intra-particle diffusion kinetic models. The equilibrium data were analyzed using Langmuir, Freundlich, Temkin and Dubinin–Radushkevich isotherm models. The thermodynamics of the adsorption was also evaluated.
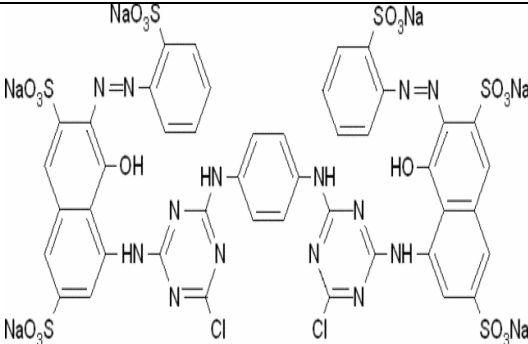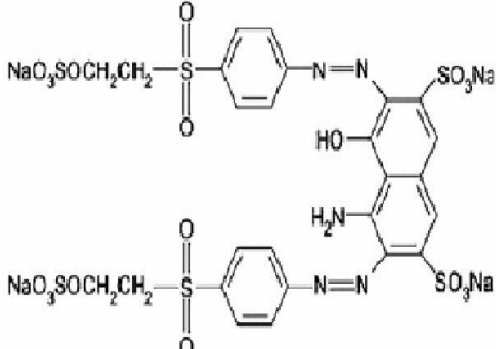
2. EXPERIMENTAL

2.1. Materials and techniques

The raw clay used in this work was collected from Nabeul region in Tunisia. In order to determine the mineralogical composition of the clay fraction XRD and IR techniques were applied to the purified clay fraction. The raw clay was purified by repeating cation exchange with NaCl solution (1N) followed by washing, sedimentation and dialysis [22]. The fine clean sediment was dried at 50°C then sieved in particles size lower than 63µm. The selected sample was indicated by NC. "p" was added to indicate the purified fraction.

Two anionic textile dyes were used in this study. The first is called Reactive Red 120 (RR120) and the second is called Reactive Blue Bezaktiv S-GLD 150 (BB150). They were provided by textile industry in the region of Nabeul. The chemical formula and some other specific characteristics of these dyes are summarized in Table 1.

X-ray diffraction (XRD) patterns of the samples were obtained using a bruker X-ray diffraction unit model with radiation Cu-Kα (1.541874 Å) at room temperature in 40kV and 20mA at a scan speed of $1.2°.min^{-1}$. Specific surface area was determined from N_2 adsorption isotherm at -196°C in a Micromeritics ASAP2010 sorptometer. Samples were out gassed prior to use at 200°C a night under vacuum. The infrared absorption spectra of a KBr pressed pellet of the powdered sample was studied in the range 4000–400 cm^{-1} using a Bruker spectrophotometer. The cation exchange capacity (CEC) was determined by the ethylene diamine-copper method.

Table1. Physicochemical characteristics of used dyes.

Name	Molecular structure	Nature	MW (g.mol⁻¹)	λmax (nm)
Reactive Red 120		Anionic	1338.04	535
Reactive Blue Bezaktiv S-GLD 150		Anionic	960	620

2.2. Adsorption tests

Stock solutions of 0.8 g.L⁻¹ of RR120 and BB150 dyes were prepared by dissolving appropriate amount of each dye in distilled water and the used concentrations were obtained by dilution. Adsorption experiments were conducted at a constant agitation speed of 450 rpm by varying the pH of solution from 3 to 9, the adsorbent dosage from 0.3 to 6 g.L⁻¹, the contact time from 10 to 130 min, the initial dyes concentrations from 20 to 150 mg.L⁻¹ and the temperature from 20 to 50°C. The pH was adjusted to a given value by addition of HCl (1 N) or NaOH (1 N) and was measured using a CRISON CLP21 pH-Meter. The temperature was controlled using a thermostatically controlled incubator.

After each adsorption experiment completed, solid and liquid phases were separated by centrifugation at 4000 rpm for 15 min. The supernatants were analyzed for residual dye concentrations by a Perkin Elmer LAMBDA 24 spectrophotometer.

The adsorbed quantity was calculated using the following equations:

$$q = (C_0 - C)\frac{V}{m} \tag{1}$$

where q (mg.g⁻¹) is dye adsorbed quantity per unit mass of adsorbent, C_0 (mg.L⁻¹) is the initial dye concentration, C (mg.L⁻¹) is the residual dye concentration, m (g) is the mass of used adsorbent and V (L) is the volume of the aqueous solution.

2.3. Equilibrium isotherm modeling

The equilibrium data were fitted using Langmuir [23,24], Freundlich [25-26], Temkin [27-29] and Dubinin–Radushkevich isotherm models [30-33].

2.3.1. Langmuir model

Langmuir isotherm assumes monolayer adsorption onto a surface containing a finite number of adsorption sites. The model assumes uniform energies of adsorption onto the surface and no transmigration of adsorbate in the plane of the surface. Based upon these assumptions, Langmuir represented the following equation:

$$q_e = \frac{Q_0 K_L C_e}{1 + K_L C_e} \tag{2}$$

Langmuir adsorption parameters were determined by transforming equation (2) into its linear form:

$$\frac{1}{q_e} = \frac{1}{Q_0} + \frac{1}{Q_0 K_L} \times \frac{1}{C_e} \tag{3}$$

Where C_e is the dye concentration at equilibrium (mg.L^{-1}), q_e is the dye adsorbed amount at equilibrium (mg/g), Qo is the maximum monolayer coverage capacity (mg.g^{-1}) and K_L is the Langmuir equilibrium constant (L.mg^{-1}).

2.3.2. Freundlich model

Freundlich adsorption isotherm is commonly used to describe the adsorption characteristics for the heterogeneous surface. Its equation is also applicable to multilayer adsorption and is expressed by equation (4):

$$q_e = K_F \, C_e^{\frac{1}{n}} \tag{4}$$

Where K_f is the Freundlich constant (mg$^{1-1/n}$.L$^{1/n}$.g^{-1}) and n is the adsorption intensity.

Freundlich adsorption parameters were determined using logarithmic form of equation (4):

$$ln q_e = ln K_F + \frac{1}{n} ln C_e \tag{5}$$

2.3.3. Temkin model

Derivation of temkin isotherm supposes that the decrease of adsorption heat is linear rather than logarithmic and that the adsorption is characterized by a uniform distribution of the bond energies up to a certain maximum binding energy. The model is given by the following equation:

$$q_e = \frac{RT}{b_T} Ln K_T + \frac{RT}{b_T} Ln C_e \tag{6}$$

Where b_T is Temkin isotherm constant, R is the universal gas constant (8.314 J.mol^{-1}.K^{-1}) and T is the absolute temperature (K). Temkin adsorption parameter, b_T (J.mol^{-1}.g.mg^{-1}), was determined from the slope and intercept of q_e vs LnCe plot.

2.3.4. Dubinin-Radushkevich model

Dubinin–Radushkevich isotherm is generally applied to express the adsorption mechanism with a Gaussian energy distribution onto a heterogeneous surface. The model has often successfully fitted high solute activities and intermediate range of concentrations data well. The model is given by the following equation:

$$q_e = q_D \exp\left(-B_D \left[RT Ln(1 + 1/C_e)\right]^2\right) \tag{7}$$

Where, B_D is a constant related to adsorption energy and q_D is the theoretical isotherm saturation capacity (mg/g). The linear form of equation (7) is:

$$Ln q_e = Ln q_D - B_D \left[RT Ln(1 + 1/C_e)\right]^2 \tag{8}$$

Dubinin–Radushkevich adsorption parameters were determined from the slope and intercept of $Ln q_e$ vs $[RT Ln(1+1/Ce)]^2$ plot.

The apparent adsorption energy (E_D) can be computed using equation (9):

$$E_D = \sqrt{1/2B_D} \tag{9}$$

2.4. Adsorption kinetic

Kinetic study of the adsorption process provides information on the mechanism adsorption and the transfer mode of the solutes from the liquid phase to the solid phase.

The procedure of the kinetic adsorption study was identical to the adsorption equilibrium study where the aqueous samples were withdrawn at different time intervals and the concentrations of dyes were similarly measured. The dye adsorbed amount, q_t (mg.g^{-1}), at time t was calculated by:

$$q_t = (C_0 - C_t) \frac{V}{m} \tag{10}$$

where C_t (mg.L^{-1}) is the dye concentrations of the liquid phase at time t.

The kinetics data were fitted using pseudo-first-order, pseudo-second-order and intra particle diffusion models.

2.4.1. Pseudo-first order model

It has been assumed that in this model constant adsorption rate k_1 (min^{-1}) at time t is proportional to the difference between the adsorbed amount at equilibrium, q_e, and the adsorbed amount at this moment, q_t, and that the adsorption is reversible [34]. Constant adsorption rate is deducted from the model established by Lagergren and coll. [35].

The kinetic law equation is:

$$ln(q_e - q_t) = ln(q_e) - k_1 t \tag{11}$$

2.4.2. Pseudo-second order model

The equation of the pseudo-second order is often used with success to describe the kinetics of the binding reaction of the pollutants on the adsorbent [36]. This model allows the characterization of the kinetics of adsorption taking into account both the case of a fast fixation of solutes on the most reactive sites and that of a slow fixation on sites with low energy.

The kinetic law equation is:

$$\frac{t}{q_t} = \frac{1}{k_2 q_e^2} + \frac{t}{q_e} \tag{12}$$

where k_2 (g.mg^{-1}.min^{-1}) is the constant adsorption rate of pseudo second-order equation.

2.4.3. Intra particle diffusion model

Intra particle diffusion model was proposed by Weber and Morris [37]. The molecule is assumed to migrate by diffusion into the liquid and enter the pores of the solid phase.

The possibility of intra- particle diffusion was explored by using the following equation [38]:

$$q = k_{id} \, t^{0.5} + I \tag{13}$$

where k_{id} is the intra-particle diffusion constant rate (mg.g^{-1}.min$^{-1/2}$) and I (mg.g^{-1}) is a constant which gives information about the thickness of boundary layer.

3. RESULTS AND DISCUSSION

3.1. Characterization of the clay sample

The identification of the clay mineral has been based on previous studies [38-41]. According to the diffractogram of the raw clay fraction (Fig.1a) the quartz (reflections at 4.26Å and 3.34Å) and the calcite (reflections at 3.02Å and 2.86Å) are the essential impurities in this clay. After purification these reflections disappear (Fig.1b).

The X-ray patterns of the purified clay fraction (Fig.2-a-b-c) show reflections at 7.17Å and 3.58Å which disappears after heating at 550°C and persist after treatment with ethylene glycol. These reflections confirm the presence of the kaolinte phase. The peaks at 9.98Å, 4.99Å and 3.33Å are detected in all the samples; they are due to the presence of illite phase.

The infrared spectrum of NCp (Fig.3b) shows:

- bands at 697 cm^{-1} and 921 cm^{-1} indicating the presence of kaolinite. They are attributed to Al-Al-OH bending vibration.
- bands at 3430 cm^{-1} and 1630 cm^{-1} corresponding, respectively, to the stretching and bending vibration of water used in hydration of clay.
- bands in 3720-3645 cm^{-1} region corresponding to the stretching vibration of hydroxyl groups.
- band with high intensity centered at 1028 cm^{-1} characteristic of the SiO_2 stretching vibration of the clay. Bending vibrations appear at 546 cm^{-1} for Si-O-Al and at 471 cm^{-1} for Si-O-Si.

The NC infrared spectrum (Fig.3a) contains additional bands at 800 cm^{-1} reveling the presence of quartz and at 1462 cm^{-1} corresponding to the carbonate. These bands disappear after purification (Fig.3b).

The chemical composition of the raw clay is indicated on table 2. The presence of potassium (1.161%) confirms the presence of illite in the clay fraction.
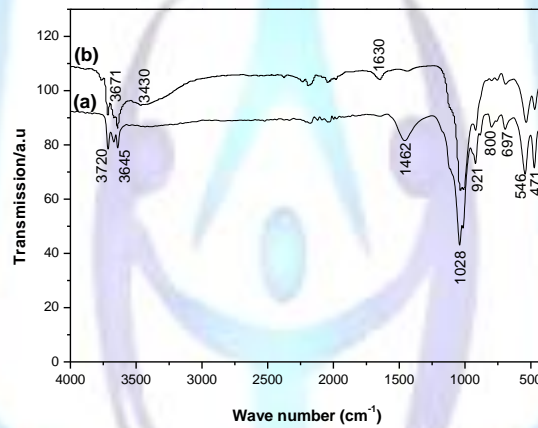
The cationic exchange capacity of the raw clay is found to be equal to 74.85 meq per 100g of fired clay. The BET specific surface of the raw clay is equal to 23.26 m^2.g^{-1} and the average pore diameter is of 130.105Å.
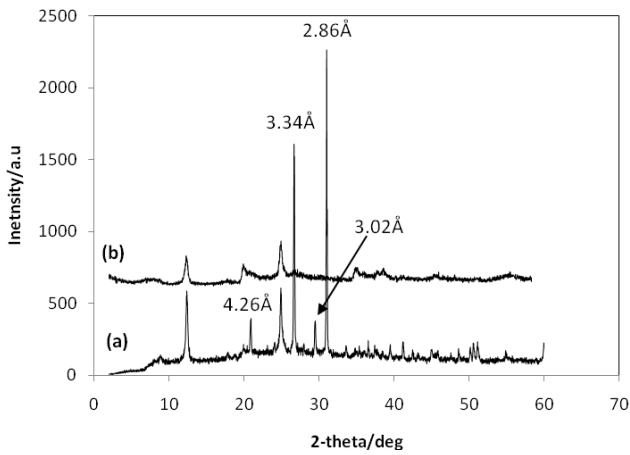
Figure 1: powder XRD patterns of NC (a) and NCp (b)
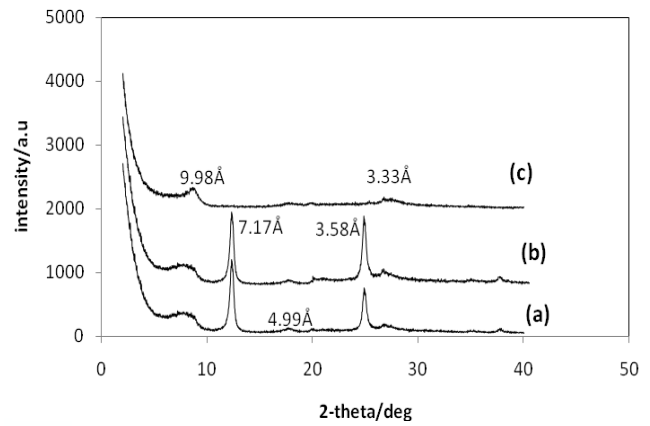
Figure 2: XRD patterns of NCp (a) dried in air (b) treated with ethylene glycol and (c) calcined at 500°C

Figure 3: IR spectra of NC (a) and NCp (b)

Table 2: chemical analysis of NC and NCp

Oxide	% in weight
SiO_2	37.50
Al_2O_3	17.21
Fe_2O_3	3.343
CaO	12.83
MgO	6.183
SO_3	0.875
K_2O	1.161
P_2O_5	0.1169
Na_2O	0.157
Loss on ignition	19.85
total	98.96

3.2. Effect of pH on the adsorption dyes

Adsorption process depends strongly on pH of the liquid phase [42]. This parameter can affect at the same time the surface charge of the adsorbent, the ionization degree of the materials present in the solution, the dissociation of functional groups on the active sites of the sorbent and also the solution dye chemistry [43]. Here, we investigated the effect of four initial solution pH (i.e., 3, 5, 7 and 9) on the removal rate of mentioned dyes. In this range the utilized dyes do not altered [44].

In Fig.4 are shown the changes observed in the adsorption of RR120 and BB150 by raw clay. It is clear that the adsorption of the anionic dyes is highly dependent on pH. The maximum of adsorption, for the two dyes, was obtained at pH = 3. When pH increases, upto pH = 7, the capacity of adsorption decreases drastically which can be explained by the increase of the repulsive forces between surface functional groups of both, the clay (hydroxyle groups OH^-) phase and dyes molecules existing mainly as anion form.

At basic pH, despite the presence of OH^- ions, we find that the adsorption capacity is higher compared to neutral pH, so we can say that there is always an attraction between the dyes and the clay. The repulsion between the OH^- ions and dyes anions decreases.
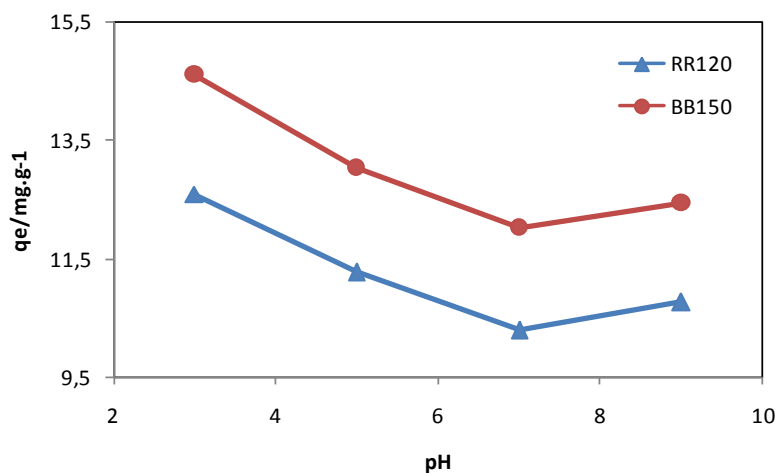

Figure 4: Effect of pH on the adsorption of RR120 and BB150 dyes by NC

3.3. Effect of initial dye concentration

Here, experiments were carried out at different initial concentrations of dyes from 20 to 150 mg.L^{-1} and at natural pH conditions. Corresponding curves are shown in Fig.5. According to the classification of Sposito [45] adsorption isotherms are of L-type which is characterized by a slope increasing with the concentration of the substance in solution. This is the result of a relatively high affinity for the solid phase to the adsorbed substance, coupled with a decrease in the number of adsorption sites. The amounts of dyes removed by the raw clay are 11.76 mg g^{-1} for RR120 and 14.76 mg.g^{-1} for BB150.
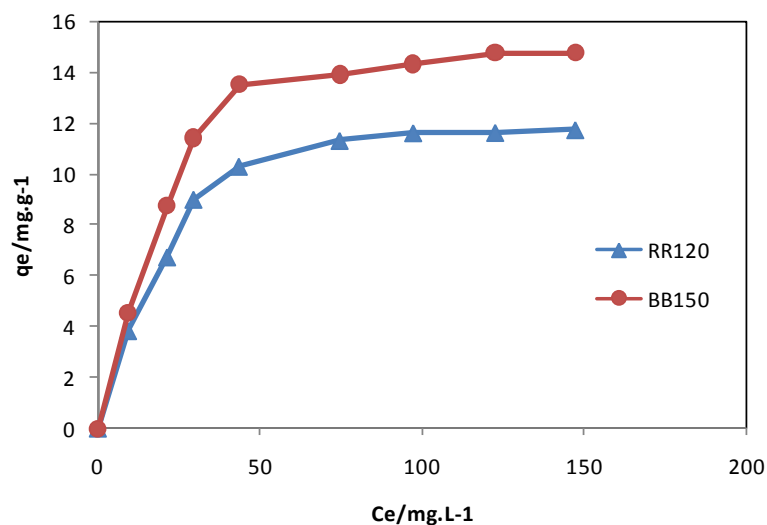

Figure 5: Effect of initial RR120 and BB150 concentration on their adsorption by NC

3.4. Effect of contact time

Here, adsorption experiments were conducted at different contact times varying from 10 to 130 min and at natural pH. The initial concentration of dyes was fixed at 80mg.L^{-1}. Corresponding curves are shown in Fig.6. The adsorption capacity of dyes increases rapidly and linearly with time contact up to 30 min. Between 30 min and 50 min adsorption rate decreases. From 50min of time contact, the adsorption capacity reaches the maximum (8.64 mg.g^{-1} for RR120 dye and 14 mg.g^{-1} for BB150 dye) and becomes independent of contact time.

The rapid adsorption during the first 30 min can be explained by the abundant availability of active sites on the clay surface, but, with the gradual occupancy of these sites, the adsorption became less efficient.
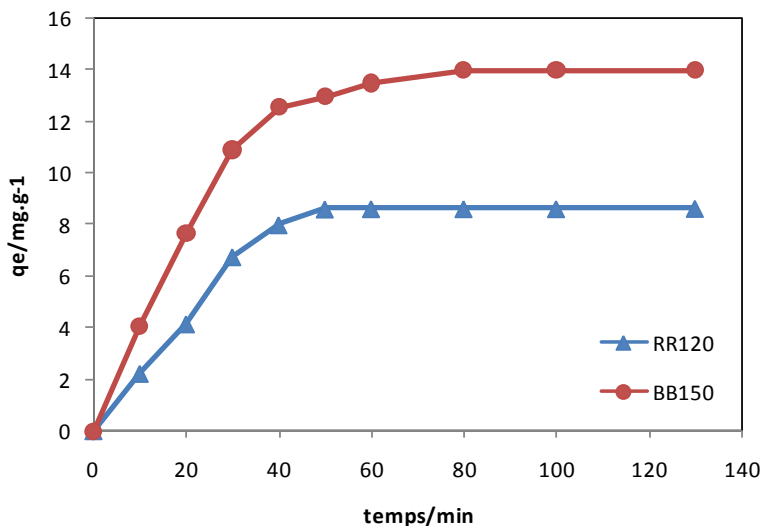
Figure 6: Effect of contact time on adsorption of RR120 and BB150 by NC

3.5. Adsorption isotherms

Fig.7 shows Langmuir, Freundlich, Temkin and Dubinin – Radushkevich isotherms for both dyes. The characteristic parameters of the different models as well as the correlation coefficients R^2 are listed in Table 3. The values of the regression coefficients indicate that the adsorption process, for both dyes, is described in a favorable manner by the Langmuir isotherm model.

Table 3. Langmuir, Freundlich, Temkin and Dubinin-Radushkevich isotherm constants for the adsorption of RR120 and BB150 by NC.

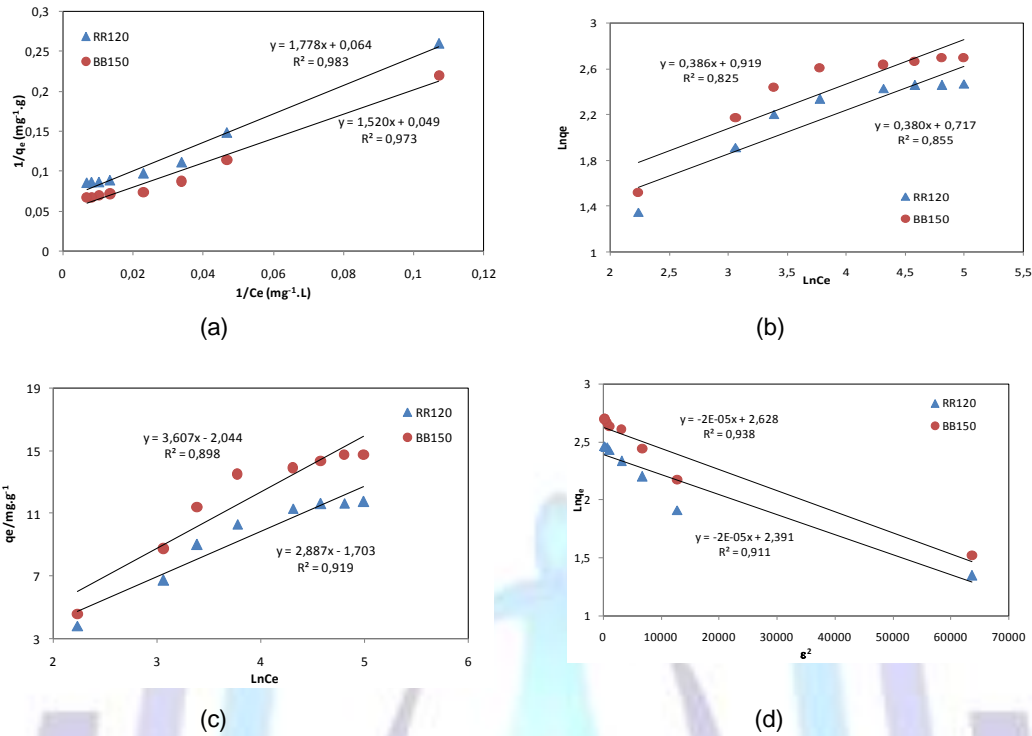| dyes	Langmuir parameters			Freundlich parameters		
	K_L	Q_0	R^2	$1/n$	K_F	R^2
RR120	0.036	15.62	0.983	0.380	2.05	0.855
BB150	0.032	20.40	0.973	0.386	2.50	0.825
	Temkin parameters			Dubinin – Radushkevich parameters			
	K_T	b_T	R^2	q_D	B_D	E_D	R^2
RR120	0.555	858.18	0.919	10.92	2.10^{-5}	0.158	0.911
BB150	0.567	686.87	0.898	13.84	2.10^{-5}	0.158	0.938

(a)

(b)

(c)

(d)

Figure 7: Langmuir (a), Freundlich (b), Temkin (c) and Dubinin–Radushkevich (d) adsorption isotherms

3.6. Effect of temperature and thermodynamic study

Adsorption is a phenomenon that may be exothermic or endothermic depending on the adsorbent material and the nature of the adsorbed molecules [46]. In order to understand the thermodynamic phenomenon of adsorption of both studied dyes by the raw clay, we performed adsorption experiments by varying the temperature of the colored solutions from 20 to 50°C.

The variation of quantities of RR120 and BB150 adsorbed on the clay as function of solution temperature are shown in Fig.8. The adsorbed quantity of both dyes decreases significantly with the increase in temperature from 20°C to 50°C.

From lnKc vs. 1/T curves (Fig.9), thermodynamic parameters including the change in free energy (ΔG°), enthalpy (ΔH°) and entropy (ΔS°) were calculated and used to describe thermodynamic behavior of the adsorption of RR120 and BB150 onto the raw clay. These parameters were calculated [47] by considering the following equations:

$$K_c = \frac{C_e}{C_0 - C_e} \qquad (14)$$

$$\Delta G° = -RTLn(K_c) \qquad (15)$$

$$ln(K_c) = -\frac{\Delta H°}{R} \times \frac{1}{T} + \frac{\Delta S°}{R} \qquad (16)$$

Where K_C is equilibrium constant, and T is solution temperature in Kelvin.
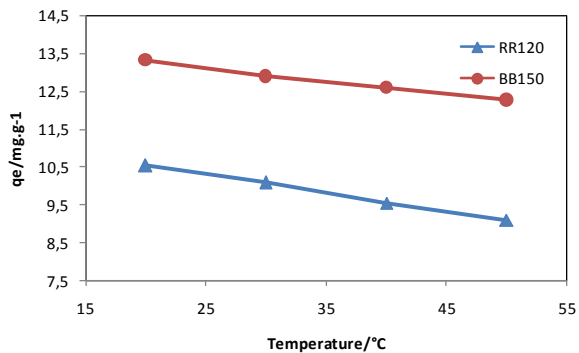

Figure 8: Effect of temperature on the adsorption equilibrium of RR120 and BB150 by NC
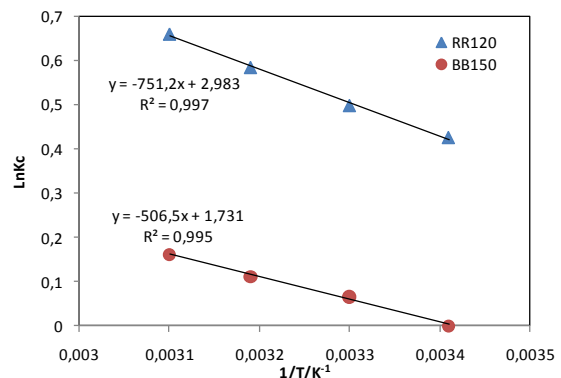

Figure 9: Thermodynamic parameters of the adsorption of RR120 and BB150 by NC

The calculated thermodynamic parameters are illustrated in Table 4. From these results, it can be concluded that, the adsorption process is endothermic in nature for both dyes BB150 and RR120. The low values of adsorption enthalpies of RR120 (6.245 kJ.mol^{-1}) and BB150 (4.211 kJ.mol^{-1}) indicate that adsorption is a physical type. Positive values of entropy show that the adsorption of both dyes on the raw clay was accompanied by an increase of disorder. This result shows that the dye molecules adsorbed on the raw clay surface are organized much random as compared with the situation in the aqueous phase.

Similarly, the negative values of ΔG° show that the process of adsorption of both dyes on the raw clay is a spontaneous process.

Table 4 Thermodynamic parameters calculated for the adsorption of dyes by NC

T(°C)	RR120			BB150		
	ΔH° (kJ.mol^{-1})	ΔS° (J.K^{-1}mol^{-1})	ΔG° (J.mol^{-1})	ΔH° (kJ.mol^{-1})	ΔS° (J.K^{-1}mol^{-1})	ΔG° (J.mol^{-1})
20			-1021.4			-5.27
30	6.245	24.80	-1269.4	4.211	14.39	-149.17
40			-1517.4			-293.07
50			-1765.4			-436.97

3.7. Adsorption kinetics

The experimental kinetic data of both dyes, calculated from Eq. (10), were correlated by three kinetic models: pseudo-first order, pseudo-second order and intra-particle diffusion (Fig.10). The calculated kinetic constants of the three kinetic models along with R^2 values are presented in Table 5. From this table we can note that the pseudo-second order kinetic model fits better the experimental results of adsorption of RR120 dye with a constant rate $k_2 = 0.004$ g.mg^{-1}.min^{-1}. Whereas adsorption of BB150 dye is best described by pseudo-first order kinetic model with a constant rate $k_1 = 0.057$ g.mg^{-1}.min^{-1}.

(a)

(b)

(c)
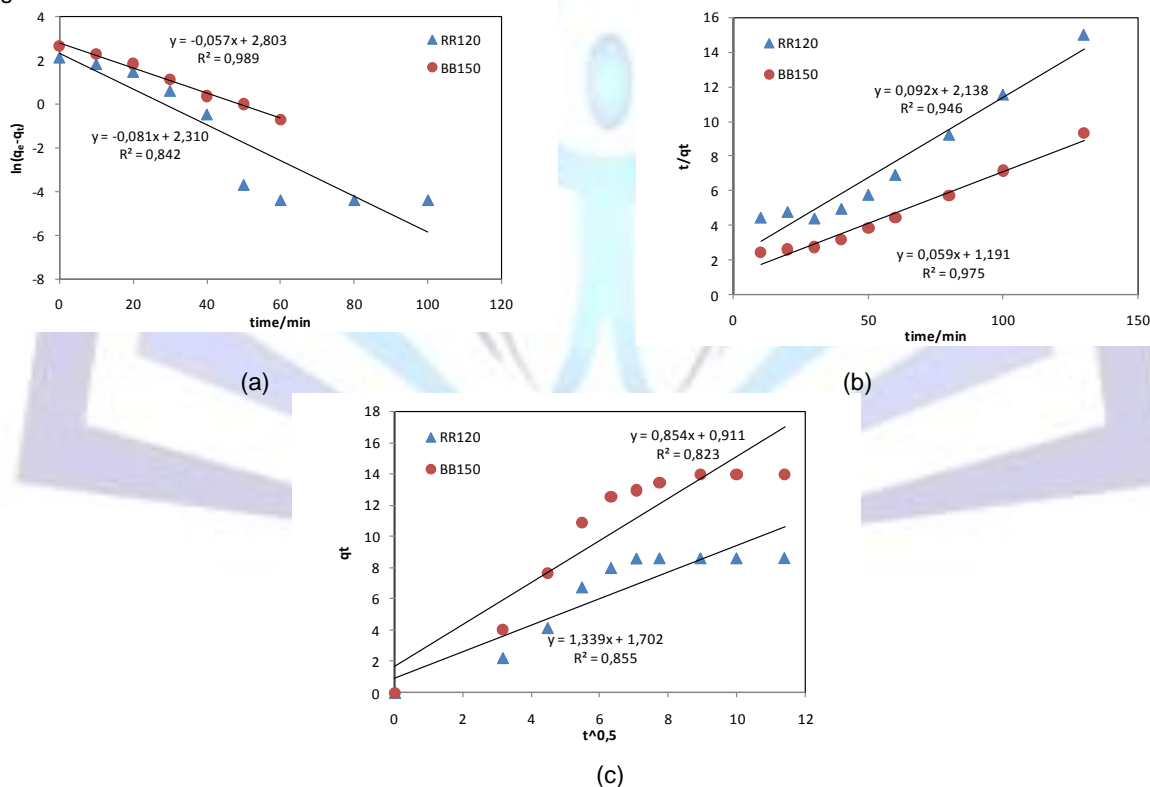
Figure 10: Pseudo- First order (a), pseudo-second order (b) and Intra particle diffusion

(c) kinetic models plots for the adsorption of BB150 and RR120 on NC

Table 5: Kinetic parameters for BB150 and RR120 dyes adsorption by NC

dyes	q_e. exp	Pseudo First-order kinetic model			Pseudo second-order kinetic model		
		k_1	q_e calc	R^2	k_2	q_e calc	R^2
RR120	8.64	0.081	10.07	0.842	0.0040	10.86	0.946
BB150	14	0.057	16.49	0.989	0.0029	16.94	0.975

dyes	q_e.exp	Intra-particule diffusion model		
		k_{id}	I	R^2
RR120	8.64	1.339	1.702	0.855
BB150	14	0.854	0.911	0.823

4. CONCLUSIONS

This work concerns the study of the potentiality of natural clay, collected near a textile industry, to remove two used textile dyes RR120 and BB150. The studied Tunisian raw clay can efficiently remove dyes from aqueous solutions. The adsorption was dependent on the pH of the aqueous solution, with high uptake of anionic dye at low pH. The adsorption isotherm could be well fitted by Langmuir equation in the case of both anionic dyes. The rise in temperature decreases the adsorbed amount of RR120 and BB150 on clay. The adsorption process is found spontaneous, endothermic and characterized by a disorder of the medium. These results suggest that the adsorption of anionic dyes by the raw clay could be physisorption. Finally, the use of Tunisian natural clay shows a greater potential for the removal of textile dyes, as no costly equipment is required.

REFERENCES

[1]   Zollinger H., 1991 Color Chemistry: Synthesis, Properties and Applications of Organic Dyes and Pigments, VCH, New York, NY,.

[2]   Gupta G.S., Prasad G. and Singh V.N., J. Environ.Sci. Health,123 (1988) 205-213.

[3]   Mazet M., Dussort O., Roger M. and Dussoubes M., Revue des sciences de l'eau, 3 (1990) 129-149.

[4]   Perineau F., Molinier J. and Gazet A., Wat. Res. 17, 5 (1983) 559-567.

[5]   Yang Y., Ladisch C. and Ladisch M. R., Enzym.Microb. Tech., 10 (1988) 632-636.

[6]   Lisheng Z. and Dobias B., Water treatment, 7 (1992) 221-232.

[7]   Barka N., Assabbane A., Ichou Y. A., Nounah A., Decantamination of textile wastewater by powdered activated carbon, J. Appl. Sci. 6 (3) (2006) 692-695.

[8]   Ahmad M.A., Puad N.A.A., Bello O.S., Kinetic, equilibrium and thermodynamic studies of synthetic dye removal using pomegranate peel activated carbon prepared by microwave-induced KOH activation, Water Resour. Ind. 6 (2014) 18-35.

[9]   Dogan M., Abak H., Alkan M., Adsorption of methylene blue onto hazelnut shell: kinetics, mechanism and activation parameters, J. Hazard. Mater. 164 (2009) 172-181.

[10]   Gurses A., Hassani A., Kıransan M., Acıslı O., Karaca S., Removal of methylene blue from aqueous solution by using untreated lignite as potential low-cost adsorbent: kinetic, thermodynamic and equilibrium approach, J. Water Process Eng. 2 (2014) 10-21.

[11]   Barka N., Assabbane A., Nounah A., Laanab L., Ichou Y. A., Removal textile dyes from aqueous solution by Natural Phosphate as new adsorbent, Desalination 235 (2009) 264-275.

[12]   Tsai F.C., Ma N., Chiang T.C., Tsai L.C., Shi J.J., Xia Y., Jiang T., Su S.K., Chuang F.S., Adsorptive removal of methyl orange from aqueous solution with crosslinking chitosan microspheres, J. Water Process Eng. 1 (2014) 2-7.

[13]   Mehrizi M.Z., Badiei A., Highly efficient removal of basic blue 41 with nanoporous silica, Water Resour. and Ind. 5 (2014) 49-57.

[14]   Dogan M., Karaoglu M.H., Alkan M., Adsorption kinetics of maxilon yellow 4GL and maxilon red GRL dyes on kaolinite, J. Hazard. Mater. 165 (2009) 1142–1151.

[15]   Barka N., Qourzal S., Assabbane A., Nounah A., Ichou Y. A., Removal of reactive yellow 84 from aqueous solutions by adsorption onto hydroxyapatite, J. Saudi Chem. Soc. 15 (2011) 263–267.

[16] Barka N., Qourzal S., Assabbane A., Nounah A., Ichou Y. A., Adsorption of Disperse Blue SBL dye by synthesized poorly crystalline hydroxyapatite, J. Environ. Sci. 20 (2008) 1268–1272.

[17] Dogan M., Alkan M., Adsorption kinetics of methyl violet onto perlite, Chemosphere 50 (2003) 517–528.

[18] Ozdemir Y., Dogan M., Alkan M., Adsorption of cationic dyes from aqueous solutions by sepiolite, Microporous Mesoporous Mater (2006) 419–427.

[19] Gemeay A.H., El-Sherbiny A.S., Zaki A.B., Adsorption and kinetic studies of the intercalation of some organic compounds onto Naþ-montmorillonite, J. Colloid Interface Sci. 245 (2002) 116–125.

[20] Barka N., Ouzaouit K., Abdennouri M., El Makhfouk M., Dried prickly pear cactus (Opuntia ficus indica) cladodes as a lowcost and eco-friendly biosorbent for dyes removal from aqueous solutions, J. Taiwan Inst. Chem. Eng. 44 (2013) 52–60.

[21] Barka N., Abdennouri M., Makhfouk M.E.L., Removal of Methylene Blue and Eriochrome Black T from aqueous solutions by biosorption on Scolymus hispanicus L.: kinetics, equilibrium and thermodynamics, J. Taiwan Inst. Chem. Eng. 42 (2011) 320–326.

[22] Van Olphan, Interscience publisher. Ny London 1963

[23] Langmuir I., the constitution and fundamental properties of solids and liquids. Part I. Solids., Journal of the American Chemical Society, 38 (1916) 2221-2295.

[24] Langmuir I., the adsorption of gases on plane surfaces of glass, mica and platinum, Journal of the American Chemical Society, 40 (1918) 1361-1403.

[25] Freundlich, H.M.F., over the adsorption in solution, J. Phys. Chem. 57 (1906) 385-471.

[26] Freundlich H.M.F., Colloid and Capillary Chemistry, Metheum, London, 1926.

[27] Temkin, M. I., adsorption equilibrium and kinetics of processes on non homogeneous and on the interactions between the adsorbed molecules, J. Phys. Chem.(USSR) 15 (1941) 296-332.

[28] Tempkin M.I., Pyzhev V., Kinetics of ammonia synthesis on promoted iron catalyst, Acta Phys. Chim. USSR 12 (1940), 327–356.

[29] Aharoni C., Ungarish M., Kinetics of activated chemisorption. Part 2.-Theoretical models, J. Chem. Soc. Faraday Trans. 73 (1977) 456–464.

[30] Dubinin M.M., the potential theory of adsorption of gases and vapors for adsorbents with energetically non-uniform surface, Chem. Rev. 60 (1960) 235–266.

[31] Dabrowski A., Adsorption-from theory to practice, Adv. Colloid Interface Sci. 93 (2001) 135–224.

[32] Gunay A., Arslankaya E., Tosun I., Lead removal from aqueous solution by natural and pretreated clinoptilolite: adsorption equilibrium and kinetics. J.Hazard. Mater. 146 (2007) 362–371.

[33] Horsfall M., spiff AI., Abia A.A., Studies on the influence of mercaptoacetic acid (MAA) modification of cassava (manihot sculenta cranz) waste biomass on the adsorption of Cu^{2+} and Cd^{2+} from aqueous solution, Korean Chemical Society; 25 (2004) 969-976.

[34] Cavet, R. (2003), Le sol - Propriétés et fonction ; Tome 1 : Edition France Agricole,

[35] Lagergren S., Zur theorie der sogenannten adsorption gelster stoffe, Kungliga Svenska Vetenskapsakademiens. Handlingar, 24 (4) (1898) 1-39.

[36] Ho Y.S., McKay G., Kinetic models for the sorption of dye from aqueous solution by wood, Process Safety and Environmental Protection, 76 (1998) 183-191.

[37] Weber J. R., Morris J.C., Kinetics of adsorption on carbon from solution, J. Sanitary Eng. Div. ASCE 89 (1963) 31–59.

[38] Farmer V.C., 1974. The infrared spectra of minerals. Mineralogical Society, London.

[39] Caillère S., Hénin S. et Rautureau M., 1982. Minéralogie des argiles. Masson, tomes I et II, 184p. et 189p.

[40] Mackenzie R.C., Heller-Kallai L., Arahman A. and Moir H.M., Interaction of Kaolinite with Calcite on Heating: III. Effect of Different Kaolinites, Clay minerals, 23, (1988) 191-203.

[41] Van Olphen H., Fripiat J.J., 1979, Data Handbook for clay minerals and other non-metallic minerals, Pergamon Press, Oxford, England, 346 pp.

[42] Aksu Z., Application of biosorption for the removal of organic pollutants: a review, process, Biochemistry 40 (2005) 997–1026.

[43] Crini G., Peindy H.N., Gimbert F., Robert C., Removal of C.I. Basic Green 4 (Malachite Green) from aqueous solutions by adsorption using cyclodextrin-based adsorbent: Kinetic and equilibrium studies, Sep. Purif. Technol. 53 (2007) 97–110.

[44] Errais E., Duplay J., Elhabiri M., Khodja M., Ocampo R., Baltenweck-Guyot R., Darragi F., Anionic RR120 dye adsorption onto raw clay: Surface properties and adsorption mechanism, Colloids and Surfaces A: Physico chemical and Engineering Aspects 403 (2012) 69-78.

[45] Sposito G., Surface reaction in natural colloidal system, Chimia 43 (1989) 169-176.

[46] Rytwo G., Ruiz-Hitzky E., Enthalpies of adsorption of methylene blue and crystal violet to montmorillonite, Journal of Thermal Analysis and Calorimetry 71 (2003) 751-759.

[47] Bouberka Z., Kacha S., Kameche M., Elmaleh S., Derriche Z., Sorption study of an acid dye from an aqueous solutions using modified clays, Journal of Hazardous Materials 119 (2005) 117-124.